Nanoelectronics and Its New Materials – A NEW ERA OF NANOSCIENCE

Nanoelectronics and Its New Materials –
A NEW ERA OF NANOSCIENCE

ZEISS
Seeing beyond

WILEY

Discover the recent advances in electronics research and fundamental nanoscience.

Nanotechnology has become the driving force behind breakthroughs in engineering, materials science, physics, chemistry, and biological sciences. In this compendium, we delve into a wide range of novel applications that highlight recent advances in electronics research and fundamental nanoscience. From surface analysis and defect detection to tailored optical functionality and transparent nanowire electrodes, this eBook covers key topics that will revolutionize the future of electronics.

To get your hands on this valuable resource and unleash the power of nanotechnology, simply download the eBook now. Stay ahead of the curve and embrace the future of electronics with nanoscience as your guide.

ZEISS

Seeing beyond

WILEY

Direct and Rapid High-Temperature Upcycling of Degraded Graphite

Tangyuan Li, Lei Tao, Lin Xu, Taotao Meng, Bryson Callie Clifford, Shuke Li, Xinpeng Zhao, Jiancun Rao, Feng Lin,* and Liangbing Hu*

Recycling the degraded graphite is becoming increasingly important, which can helped conserve natural resources, reduce waste, and provide economic and environmental benefits. However, current regeneration methods usually suffer from the use of harmful chemicals, high energy and time consumption, and poor scalability. Herein, we report a continuously high-temperature heating (≈2000 K) process to directly and rapidly upcycle degraded graphite containing impurities. A sloped carbon heater is designed to provide the continuous heating source, which enables robust control over the temperature profile, eliminating thermal barrier for heat transfer compared to conventional furnace heating. The upcycling process can be completed within 0.1 s when the degraded graphite rolls down the sloped heater, allowing us to produce the upcycled graphite on a large scale. High-temperature heating removes impurities and enhances the graphitization degree and (002) interlayer spacing, making the upcycled graphite more suitable for lithium intercalation and deintercalation. The assembled upcycled graphite||Li cell displays a high reversible capacity of ≈320 mAh g^{-1} at 1 C with a capacity retention of 96% after 500 cycles, comparable to current state-of-the-art recycled graphite. The method is a chemical-free, rapid, and scalable way to upcycle degraded graphite, and is adaptable to recycle other electrode materials.

1. Introduction

Lithium-ion batteries (LIBs) are widely used as the power source for various applications such as consumer electronics, medical devices, and electric vehicles (EVs).[1,2] Recently, the demand for LIBs has skyrocketed in the EV market with hopes that EVs will mitigate the impacts of climate change, compared to traditional gasoline-powered vehicles.[3,4] Owing to LIBs limited lifespan, there will be numerous degraded electrode materials (e.g., graphite anode and LiNi$_x$Mn$_y$Co$_z$O$_2$ cathode) and spent accessory parts (e.g., Al and Cu current collectors) when LIBs reach their end of life.[5–9] Recycling these materials is thus becoming increasingly important, which can help conserve natural resources, reduce waste, and provide economic and environmental benefits.[10–13] Currently, graphite is the most widely used anode material for LIBs.[14,15] Graphite anodes can suffer from excessive solid

T. Li, L. Xu, T. Meng, B. C. Clifford, S. Li, X. Zhao, L. Hu
Department of Materials Science and Engineering
University of Maryland
College Park, Maryland MD 20742, USA
E-mail: binghu@umd.edu

L. Tao, F. Lin
Department of Chemistry
Virginia Tech
Blacksburg, Virginia VA 24061, USA
E-mail: fenglin@vt.edu

J. Rao
Advanced Imaging and Microscopy Laboratory
Maryland Nanocenter
University of Maryland
College Park, Maryland MD 20742, USA

F. Lin
Department of Materials Science and Engineering
Virginia Tech
Blacksburg, Virginia VA 24061, USA

L. Hu
Center for Materials Innovation
University of Maryland
College Park, Maryland MD 20742, USA

**ADVANCED
SCIENCE NEWS**

www.advancedsciencenews.com

**ADVANCED
FUNCTIONAL
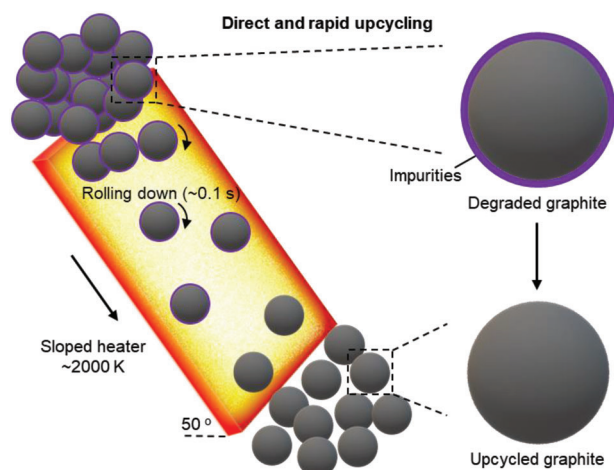MATERIALS**

www.afm-journal.de

Figure 1. Direct and rapid high-temperature upcycling of graphite anodes. Schematic of the sloped carbon paper heater, in which degraded graphite powder rapidly rolls down from top to bottom of the heated carbon paper under an inert atmosphere. The degraded graphite contains impurities such as SEI, binder, and residual electrolyte, while the sample after high-temperature upcycling shows pure graphite without impurities.

electrolyte interphase (SEI) formation and structural damage (e.g., loss of graphitization) upon long-term cycling, which reduces battery performance.[14–16] Several methods have been demonstrated to recycle used or degraded graphite (DG), including chemical and thermal treatments.[17–20] Acid leaching treatment is commonly used to remove impurities (e.g., SEI, binder, and residual electrolyte) from DG.[21,22] However, this kind of chemical processes is tedious and yields acidic wastewater, causing severe pollution. [14,15,23] Additionally, chemical treatments are limited when the goal is to recover the crystalline structure of graphite. [14,15] As for thermal treatments, furnace heating has been explored to simultaneously remove impurities and recover the crystalline structure of DG, while it is time-consuming (on the order of h) and energy-consuming.[24] Recently, a flash high-temperature recycling method has been applied to regenerate DG powders, which can greatly shorten the heating time within seconds.[25,26] However, the process is carried out in a closed environment inside a quartz tube reactor,[25,26] limiting its potential for continuous large-scale production. Therefore, there is a need to develop a fast, energy-efficient and scalable process to recycle DG from LIBs.

Herein, we report an electrified carbon heater-based process which provides continuous high-temperature heating (≈2000 K) capable of direct and rapid upcycling of DG containing impurities (e.g., SEI and binder), as shown in Figure 1. DG powders were poured on the top of the sloped carbon heater, and then rolled down from top to bottom during heating. The process only takes ≈0.1 s, which enables continuous, rapid and large-scale production of upcycled graphite (UG). As a result of this process, the impurities are effectively removed from DG, and both the carbon's degree of graphitization and the interlayer spacing of (002) are enhanced in the UG. Such a carbon structure is more favorable for lithium intercalation and deintercalation. As a demonstration, a graphite anode made of UG was fabricated and assembled into an UG‖Li battery, exhibiting a high reversible capacity

of ≈320 mAh g^{-1} at 1 C with a capacity retention of 96% after 500 cycles. Our strategy does not require the use of chemicals nor water washing and is a simple and time-saving option for upcycling DG compared to reported regeneration methods.[14,15]

2. Results and Discussion

We designed a continuous high-temperature setup to directly and rapidly upcycle DG from LIBs (see the Experimental Section and Figure 2a). The setup features a simple design of a sloped carbon paper film (thickness: 190 µm; length: 5 cm; width: 2 cm; angle: 50 ° between the sloped film and the horizontal plane), which can generate ultra-high temperatures with a stable, uniform and controlled temperature distribution by Joule heating and enable ultrafast decomposition of impurities. By pouring DG at the top of the heater, graphite powders roll down from top to bottom along the heater under gravity (no applied force) during heating. The Joule-heated carbon paper can reach a temperature as high as ≈3000 K. As a result, the decomposition of impurities occurs at a much faster rate and is completed within the 0.1 s it takes the graphite particles to roll down the electrified heater (overall reducing energy consumption). Afterward, the UG powders can be collected at the bottom of the sloped heater. In this way, we have the ability to continuously upcycle DG on a large scale. As a proof-of-concept demonstration, we successfully upcycled DG via this continuous high-temperature setup at a constant temperature of ≈1970 K. The spatial temperature distributions of the heater and graphite during upcycling were recorded using an infrared camera every 1/30 s (see the Experimental Section). The upcycling process was completed in a short time of 0.1 s (Figure 2b). The maximum temperatures of the electrified heater and graphite were ≈1970 K and ≈1530 K, respectively (Figure 2c), both of which are higher than the temperature required for complete decomposition of impurities (≈873 K, Figure S1, Supporting Information). Such high temperatures ensure the rapid decomposition/removal of impurities. The heating temperature can be adjusted up to 3000 K to further optimize the properties of the UG.

Here we used DG collected from spent 18650-type cells (see the Experimental Section). The as-obtained DG (Figure 2d, f) shows particle agglomeration due to binder use, while no particle agglomeration was observed in the UG, implying the successful removal of the binder (Figure 2e, g). We performed scanning electron microscopy-energy dispersive spectroscopy (SEM-EDS) to further reveal the elemental components of the two samples. As shown in Figure 3a, b, impurities were attached onto the surface of the DG, while the UG shows a smooth surface without impurities. The DG contains C, O, F, and P elements with an atomic percentage of 92.71 at%, 3.71 at%, 3.04 at%, and 0.54 at%, respectively (Figure 3c). After upcycling, the UG contains C, less O (only 0.1 at%) and nearly zero percent F and P (Figure 3d), similar to fresh graphite (Figure S2, Supporting Information). Fourier-transform infrared spectroscopy (FTIR) results also suggest the successful removal of O due to the disappearance of C=O vibrations (i.e., 1093 cm^{-1} and 1049 cm^{-1})[27] in the UG (Figure 3e and Figure S3, Supporting Information). In addition, we performed Inductively Coupled Plasma Mass Spectrometry and determined that the DG contained ≈0.90 wt.% Li, whereas the UG included less than 0.01 wt.% Li. This discrepancy suggests that
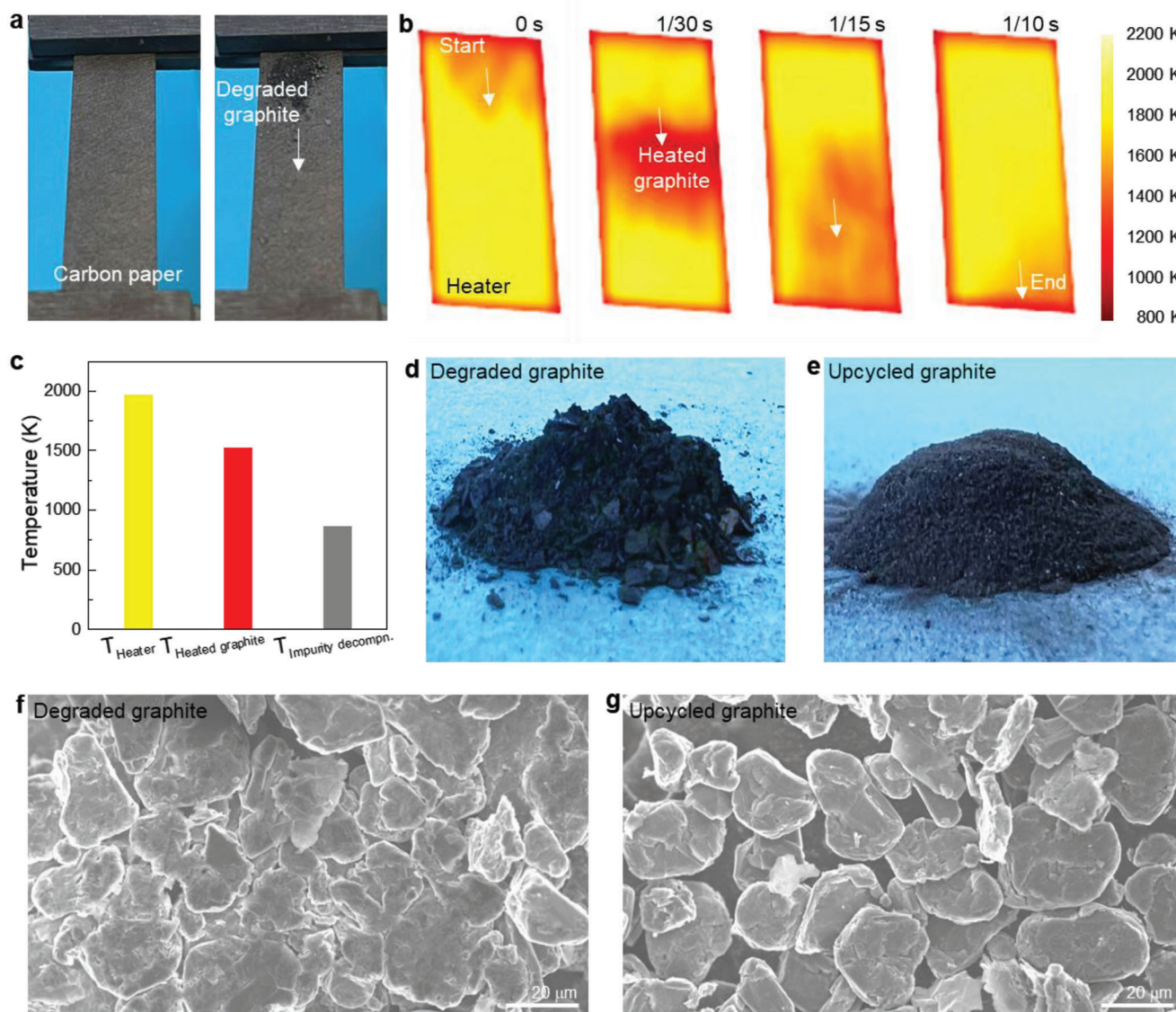
**ADVANCED
SCIENCE NEWS**

www.advancedsciencenews.com

**ADVANCED
FUNCTIONAL
MATERIALS**

www.afm-journal.de

Figure 2. Process of high-temperature upcycling and morphology of the degraded and upcycled graphite. a) Digital images of the sloped carbon paper heater, in which degraded graphite powder rapidly rolls down from the top to bottom of the heated carbon paper. b) Temperature distributions for the heated carbon heater and graphite during upcycling, collected by an infrared camera every 1/30 s. c) Temperatures of the heated carbon heater and graphite, compared to the temperature needed for complete decomposition of impurities. d, e) Digital images of d) the degraded and e) upcycled graphite. f, g) Corresponding SEM images of f) the degraded and g) upcycled graphite.

the Li ions were vaporized during the high-temperature heating process. Microscopically, the SEI layer ($\approx$40 nm) was clearly observed in the DG (Figure 3f and Figure S4, Supporting Information). In contrast, no SEI layer was found in the UG (Figure 3g), and the SEI layer (or the impurity) underwent transformation into carbon as a result of high-temperature heating (Figure S5, Supporting Information). Therefore, our high-temperature upcycling effectively promotes the carbonization and gasification of these impurities in the DG, achieving an impurity-free UG.

In addition to the successful removal of impurities, the upcycling process also recovers and improves the crystalline structure of carbon by increasing the graphitization degree and interlayer

spacing of the (002) plane. As shown in Figure 4a–b, the DG exhibits a discontinuous graphite layer and numerous defects, as evidenced by the split spots in the Fast Fourier Transform (FFT) and its corresponding inverse FFT images. The intercalation and deintercalation of lithium lead to the deterioration of the graphite structure. In contrast to the DG, the UG displays a continuous graphite layer and fewer defects, as demonstrated by the FFT and inverse FFT results (clear (002) plane). Figure 4c depicts the Raman results of the DG and UG. A fluorescence bump was found in the DG due to the existence of impurities, while the bump disappears in the UG. Typically, the D and G bands are attributed to the breathing and stretching modes of sp^2 hybridized carbon, and their intensity ratio (i.e., I_D/I_G) indicates the graphitization

**ADVANCED
SCIENCE NEWS**

www.advancedsciencenews.com

**ADVANCED
FUNCTIONAL
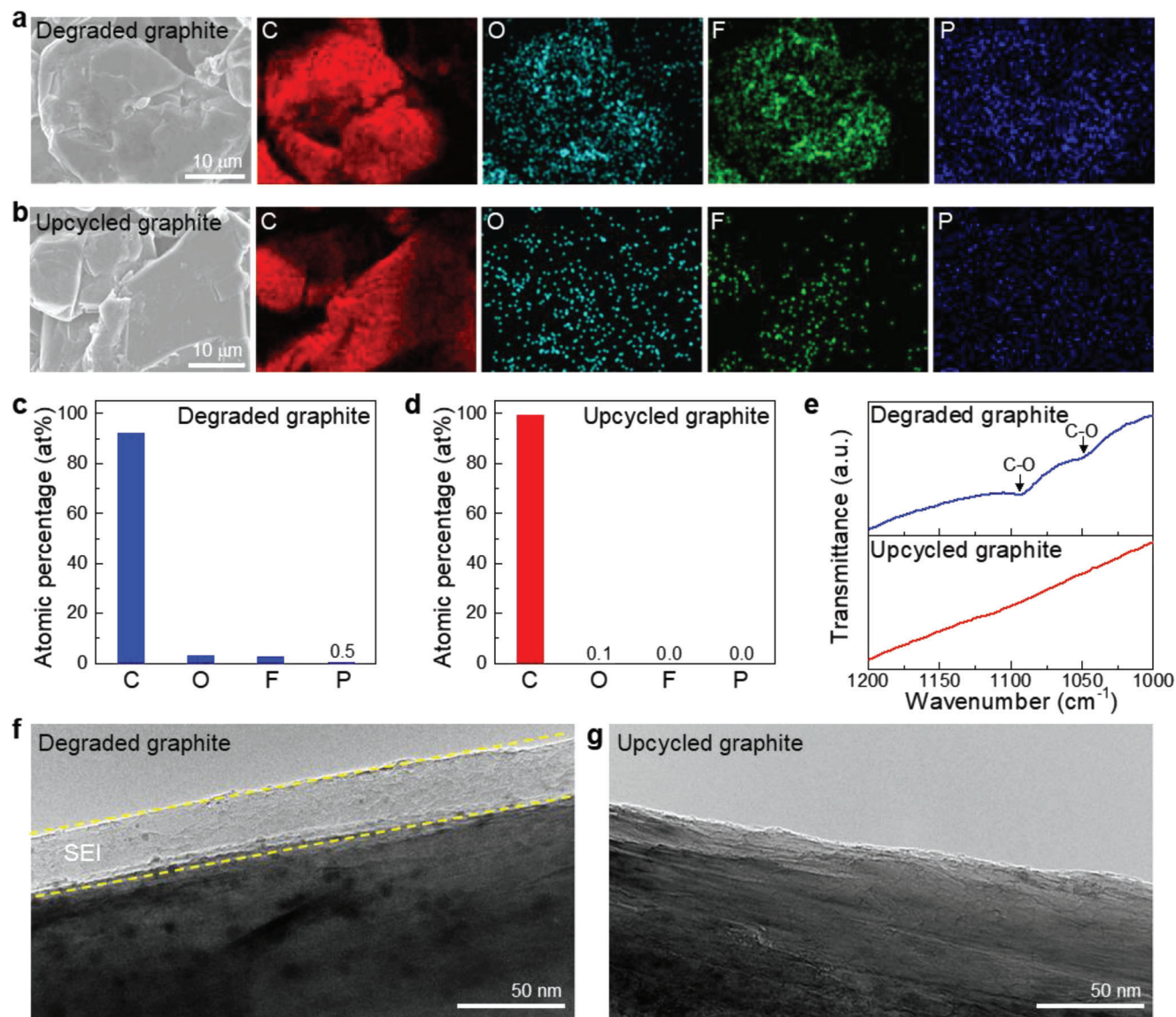MATERIALS**

www.afm-journal.de

Figure 3. Morphologies, elemental mappings and contents of the degraded and upcycled graphite. SEM images and elemental mappings of the a) degraded and b) upcycled graphite. Elemental contents of the c) degraded and d) upcycled graphite. e) FTIR spectra of the degraded and upcycled graphite. TEM images of the f) degraded (containing the SEI layer) and g) upcycled graphite.

degree of carbon, in which a high graphitization degree leads to a small I_D/I_G ratio.[28] The DG shows an I_D/I_G ratio of 0.25. In contrast, after upcycling, the I_D/I_G ratio decreased to 0.09, comparable to that of fresh graphite ($I_D/I_G = 0.10$, Figure S6, Supporting Information). Raman results show that the high-temperature treatment removes the impurities and increases the graphitization degree of carbon. In addition, compared to the DG, an increased interlayer spacing at (002) was also found in the UG. Figures 4d,e display the XRD results of DG and UG; both demonstrate typical peaks of the hexagonal phase. The (002) diffraction peak ($\approx 26°$) of the UG visibly shifts to a smaller angle when compared to DG. The Rietveld refinement for the two samples was performed using the GSAS-EXPGUI program[28] to reveal the carbon structure (Figure S7 and Table S1, Supporting Information). A hexagonal phase with a space group $P63/mmc$ was used

as an initial model.[29] The refinement results calculate the interlayer spacing at (002) of the UG as 3.370 Å, which is larger than that of the DG (3.352 Å). The increased interlayer spacing makes the UG more suitable for lithium intercalation and deintercalation.

We further investigated the electrochemical performance of the UG to highlight the effectiveness of our upcycling method. UG‖Li cells were assembled with $LiPF_6$-based electrolyte and a mass loading of 2 mg cm^{-2} (see the Experimental Section). Charge/discharge profiles of UG‖Li at a rate of 0.2 C (Figure 5a) and 1.0 C (Figure 5b and Figure S8, Supporting Information) show comparable voltage plateaus as fresh graphite (Figure S9, Supporting Information), demonstrating that our process successfully recovers the structure of DG. The removal of SEI layer was confirmed by the initial cycle performance (Figure S10,
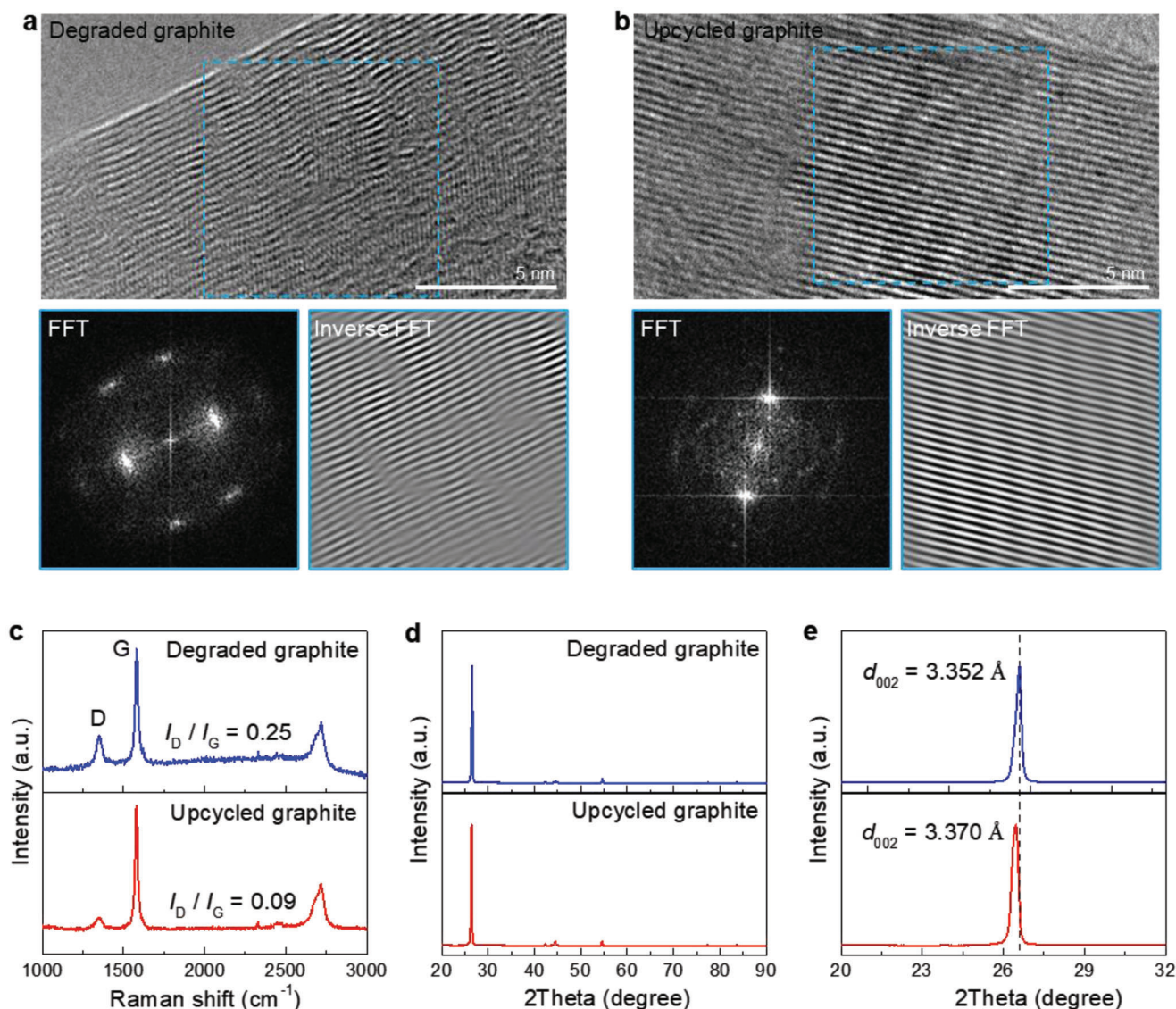
**ADVANCED
SCIENCE NEWS**

www.advancedsciencenews.com

**ADVANCED
FUNCTIONAL
MATERIALS**

www.afm-journal.de

Figure 4. Structural evolutions of degraded and upcycled graphite. HRTEM, FFT, and inverse FFT images for the a) degraded and b) upcycled graphite. The FFT and inverse FFT images were derived from the region marked by the blue dashed box in their corresponding HRTEM image. c) Raman spectra with an I_D/I_G ratio of the degraded and upcycled graphite. d, e) X-ray diffraction patterns of the degraded and upcycled graphite, showing their interlayer spacing at (002).

Supporting Information). As shown in Figure 5c, the UG||Li cell delivers an initial Coulombic efficiency of 90% at 0.2 C rather than 100%. This indicates the formation of a new SEI layer on the surface of UG, and validates that our upcycling strategy has removed the SEI layer on the surface of DG. The assembled UG||Li cells were also subjected to long-term cycling tests at different currents. After 200 cycles, the UG maintains a reversible capacity of ≈350 mAh g^{-1} at 0.2 C without capacity fading, significantly surpassing the DG (Figure S11, Supporting Information). At a higher rate of 1 C, the UG displays a high reversible capacity of ≈320 mAh g^{-1} with a capacity retention of 96% after 500 cycles (Figure 5d). Such long-term cycling stability of the UG is almost indistinguishable from that of fresh graphite and is comparable with that of the state-of-the-art recycled graphite reported in literature

(Figure 5e and Table S2, Supporting Information).[30–32] Battery performance results suggest that our rapid high-temperature heating successfully upcycled the DG. It is worth noting that our work significantly decreases the processing time to ≈0.1 s, and the continuous heating setup is advantageous for large-scale production of UG, compared to other fast heating methods.[25,26,33]

3. Conclusion

In summary, we developed a continuous high-temperature heating method to upcycle DG, capable of removing impurities such as SEI layers and binders, and recovering the graphite crystalline structure. A sloped carbon heater was used to provide a continuous heating source, which can be easily adjusted to achieve
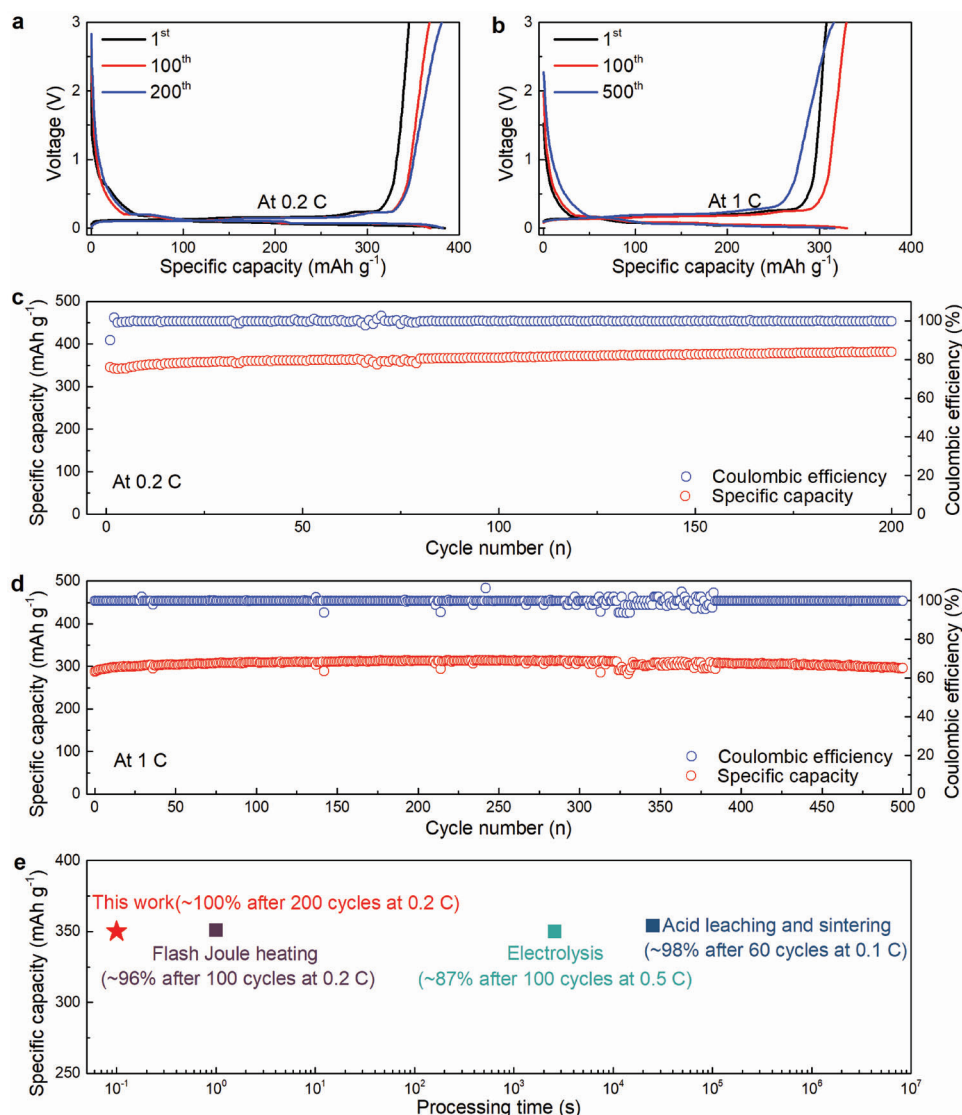
**ADVANCED
SCIENCE NEWS**

www.advancedsciencenews.com

**ADVANCED
FUNCTIONAL
MATERIALS**

www.afm-journal.de

Figure 5. Battery performance of the upcycled graphite. Voltage profiles of the UG||Li cell at current densities of a) 0.2 C and b) 1 C. Long-term cycling performance of the UG||Li cell at current densities of c) 0.2 C and d) 1 C. e) Comparison of the specific capacity and capacity retention of the recycled graphite achieved by several representative methods including our rapid upcycling, flash Joule heating,[30] electrolysis,[31] and acid leaching and sintering,[32] and their processing time for recycling the degraded graphite.

different temperatures. By pouring the DG at the top of the sloped heater, the powders roll down from the top to bottom of the heater during heating at ≈2000 K. The upcycling process is fast (only ≈0.1 s) and enables the DG to be heated continuously. The resulting UG displays no residual impurities, a high-degree graphitization and an increased interlayer spacing at (002), compared to the DG, which is more suitable for lithium intercalation and deintercalation. When using UG in an assembled UG||Li cell, the battery demonstrates a high reversible capacity of ≈320 mAh g^{-1} at 1 C with a capacity retention of 96% after 500 cycles. This work presents a promising scalable method to directly and rapidly upcycle the DG from spent LIBs and can potentially be applied to other cathode/anode materials, significantly reducing time consumption and enhancing production rate.

4. Experimental Section

Materials: Natural graphite (i.e., fresh graphite) was provided by the Cell Analysis, Modeling, and Prototyping (CAMP) Facility in Argonne National Lab. The degraded graphite was collected from the spent 18650-type cells. We mechanically scraped the degraded graphite off the Cu current collector. Then, the degraded graphite was directly upcycled by rapid high-temperature heating, as described in the following.

Rapid and Direct High-Temperature Upcycling: The upcycling setup features a simple design of a sloped carbon paper film (AvCarb MGL190, FuelCellStore) which was clamped using two graphite plates at the top and bottom sides. The two sides were connected to a DC power source (MP10050D, StarPower). The carbon paper heater was continuously Joule-heated at a constant temperature under an Ar-filled glovebox to provide the heating source for upcycling the degraded graphite. The heater was able to achieve different temperatures by tuning the voltage applies to the carbon film. The degraded graphite powders were poured on the top of the

heated heater and allowed to roll down from top to bottom under gravity during heating. This process was completed within 0.1 sec. The degraded graphite was continuously poured on the top of the heated heater and upcycled to achieve the upcycled graphite at the bottom of the heater.

Characterization: We used an infrared camera VarioCAM HDx head 600 (7.5–14 µm) with a resolution of 640 × 480 IR pixels and an infrared image rate of 30 Hz to collect the temperature mapping of the heated heater and graphite, in which the IR camera was placed 20 cm away from the heating setup. Thermal gravimetric analysis (TGA, Discovery SDT 650, TA Instruments) was performed to investigate the decomposition temperature of the impurities in the degraded graphite, in which we loaded 20–30 mg degraded graphite into the TGA instrument in Argon atmosphere with a heating rate of 5 °C/min to 1173 K. The morphologies and elemental mappings of the fresh, degraded, and upcycled graphite were revealed using scanning electron microscopy (SEM) and energy dispersive spectroscopy (EDS) equipped on a Hitachi SU-70 Schottky field-emission gun (SU-70, Hitachi, Tokyo, Japan). The microstructure of the degraded and upcycled graphite was studied by using high-resolution transmission electron microscopy (HRTEM, JEM 2100F). Fourier-transform infrared spectroscopy (FTIR) spectra of the fresh, degraded, and upcycled graphite were recorded using a Nexus 670 FTIR spectrometer. Raman measurements of the fresh, degraded, and upcycled graphite were performed on a Horiba Jobin-Yvon using a 532 nm laser. X-ray diffraction (XRD) spectra of the fresh, degraded, and upcycled graphite were collected from 20° to 90° using an automated diffractometer (D8 Advance, Bruker, Karlsruhe, Germany) with Cu Kα radiation at room temperature. Elemental quantitation for the degraded and upcycled graphite was conducted by using inductively coupled plasma mass spectrometry (ICP-MS, PerkinElmer NexION 300D). The two samples were digested in concentrated nitric acid for 24 h at a concentration of 1 mg/mL, and diluted 20-fold in high-purity water to reach a concentration of 5% nitric acid, ready to be tested by ICP-MS. The degraded graphite contained ≈0.90 wt.% Li and ≈0.59 wt.% Cu, whereas the upcycled graphite included less than 0.01 wt.% of both Li and Cu.

Graphite||Li Cell Assembly and Testing: The fresh, degraded, and upcycled graphite anodes were prepared by mixing fresh graphite, degraded, or upcycled graphite, carbon black, and PDVF (at a mass ratio of 92:3:5) in the NMP solution, stirring to form a homogenous slurry and then casting on Cu foil. The prepared graphite anode was punched into φ12 mm disks and dried overnight in a vacuum oven at 393 K. The mass loading of the active material is close to 2.0 mg/cm^{-2}. The electrolyte is 1 M LiPF$_6$ dissolved into a mixture of ethylene carbonate and ethyl methyl carbonate at a ratio of 3/7 by weight. The fresh graphite||Li or UG||Li cell was assembled from the fresh graphite or UG anode, 60 µL electrolyte, Celgrad 2325 separator, and fresh Li foil in an Ar-filled glovebox with H$_2$O and O$_2$ level≤1 ppm. The cell was tested at room temperature using a LAND battery test system (CT 2001A) in a voltage range of 0.005–3 V (vs Li$^+$/Li).

Supporting Information

Supporting Information is available from the Wiley Online Library or from the author.

Conflict of Interest

The authors declare no conflict of interest.

Author Contributions

T.L. and L.T. contributed equally to this work. L. Hu, F. Lin, and T. Li designed the experiments. T. Li performed high-temperature upcycling. T. Li, S. Li, T. Meng, and J. Rao conducted materials characterization. X. Zhao carried out the temperature measurement. L. Tao performed the battery test. T. Li, L. Tao, L. Xu, and B. C. Clifford collectively wrote the paper. All authors commented to the final manuscript.

Data Availability Statement

The data that support the findings of this study are available from the corresponding author upon reasonable request.

[1] J. Lu, Z. Chen, F. Pan, Y. Cui, K. Amine, *Electrochem. Energy Rev.* **2018**, *1*, 35.
[2] T. M. Gür, *Energy Environ. Sci.* **2018**, *11*, 2696.
[3] Y. Tian, G. Zeng, A. Rutt, T. Shi, H. Kim, J. Wang, J. Koettgen, Y. Sun, B. Ouyang, T. Chen, Z. Lun, Z. Rong, K. Persson, G. Ceder, *Chem. Rev.* **2021**, *121*, 1623.
[4] Z. Yang, H. Huang, F. Lin, *Adv. Energy Mater.* **2022**, *12*, 2200383.
[5] G. Harper, R. Sommerville, E. Kendrick, L. Driscoll, P. Slater, R. Stolkin, A. Walton, P. Christensen, O. Heidrich, S. Lambert, A. Abbott, K. Ryder, L. Gaines, P. Anderson, *Nature* **2019**, *575*, 75.
[6] P. Xu, Q. Dai, H. Gao, H. Liu, M. Zhang, M. Li, Y. Chen, K. An, Y. S. Meng, P. Liu, Y. Li, J. S. Spangenberger, L. Gaines, J. Lu, Z. Chen, *Joule* **2020**, *4*, 2609.
[7] M. Chen, X. Ma, B. Chen, R. Arsenault, P. Karlson, N. Simon, Y. Wang, *Joule* **2019**, *3*, 2622.
[8] Z. J. Baum, R. E. Bird, X. Yu, J. Ma, *ACS Energy Lett.* **2022**, *7*, 712.
[9] Q. Dong, T. Li, Y. Yao, X. Wang, S. He, J. Li, J. Luo, H. Zhang, Y. Pei, C. Zheng, M. Hong, H. Qiao, J. Gao, D. Wang, B. Yang, L. Hu, *Joule* **2020**, *4*, 2374.
[10] Y. Tao, C. D. Rahn, L. A. Archer, F. You, *Sci. Adv.* **2021**, *7*, eabi7633
[11] M. Fan, X. Chang, Q. Meng, L. Wan, Y. Guo, *SusMat* **2021**, *1*, 241.
[12] J. J. Roy, S. Rarotra, V. Krikstolaityte, K. W. Zhuoran, Y. D. I. Cindy, X. Y. Tan, M. Carboni, D. Meyer, Q. Yan, M. Srinivasan, *Adv. Mater.* **2022**, *34*, 2103346.
[13] H. Xie, M. Hong, E. M. Hitz, X. Wang, M. Cui, D. J. Kline, M. R. Zachariah, L. Hu, *J. Am. Chem. Soc.* **2020**, *142*, 17364.
[14] H. Zhang, Y. Yang, D. Ren, L. Wang, X. He, *Energy Storage Mater.* **2021**, *36*, 147.
[15] S. Natarajan, V. Aravindan, *Adv. Energy Mater.* **2020**, *10*, 2002238.
[16] K. Xu, *J. Power Sources* **2023**, *559*, 232652.
[17] B. Markey, M. Zhang, I. Robb, P. Xu, H. Gao, D. Zhang, J. Holoubek, D. Xia, Y. Zhao, J. Guo, M. Cai, Y. S. Meng, Z. Chen, *J. Electrochem. Soc.* **2020**, *167*, 160511.
[18] Y. Gao, J. Zhang, H. Jin, G. Liang, L. Ma, Y. Chen, C. Wang, *Carbon N. Y.* **2022**, *189*, 493.
[19] H. Yu, H. Dai, Y. Zhu, H. Hu, R. Zhao, B. Wu, D. Chen, *J. Power Sources* **2021**, *481*, 229159.
[20] X. Zhu, J. Xiao, Q. Mao, Z. Zhang, Z. You, L. Tang, Q. Zhong, *Chem. Eng. J.* **2022**, *430*, 132703.
[21] X. Ma, M. Chen, B. Chen, Z. Meng, Y. Wang, *ACS Sustainable Chem. Eng.* **2019**, *7*, 19732.
[22] J. Yang, E. Fan, J. Lin, F. Arshad, X. Zhang, H. Wang, F. Wu, R. Chen, L. Li, *ACS Appl. Energy Mater.* **2021**, *4*, 6261.

ADVANCED
SCIENCE NEWS

www.advancedsciencenews.com

ADVANCED
FUNCTIONAL
MATERIALS

www.afm-journal.de

[23] H. Wang, Y. Huang, C. Huang, X. Wang, K. Wang, H. Chen, S. Liu, Y. Wu, K. Xu, W. Li, *Electrochim. Acta* **2019**, *313*, 423.

[24] C. Yi, Y. Yang, T. Zhang, X. Wu, W. Sun, L. Yi, *J. Clean. Prod.* **2020**, *277*, 123585.

[25] P. Huang, R. Zhu, X. Zhang, W. Zhang, *J. Environ. Sci. Heal. Part A* **2022**, *57*, 33.

[26] S. Dong, Y. Song, K. Ye, J. Yan, G. Wang, K. Zhu, D. Cao, *EcoMat* **2022**, *4*, e12212.

[27] V. Ţucureanu, A. Matei, A. M. Avram, *Crit. Rev. Anal. Chem.* **2016**, *46*, 502.

[28] S. Reich, C. Thomsen, *Philos. Trans. R. Soc. A* **2004**, *362*, 2271.

[29] P. Trucano, R. Chen, *Nature* **1975**, *258*, 136.

[30] W. Chen, R. V. Salvatierra, J. T. Li, C. Kittrell, J. L. Beckham, K. M. Wyss, N. La, P. E. Savas, C. Ge, P. A. Advincula, P. Scotland, L. Eddy, B. Deng, Z. Yuan, J. M. Tour, *Adv. Mater.* **2022**, *35*, 2207303.

[31] N. Cao, Y. Zhang, L. Chen, W. Chu, Y. Huang, Y. Jia, M. Wang, *J. Power Sources* **2021**, *483*, 229163.

[32] W. Fan, J. Zhang, R. Ma, Y. Chen, C. Wang, *J. Electroanal. Chem.* **2022**, *908*, 116087.

[33] J. Luo, J. Zhang, Z. Guo, Z. Liu, S. Dou, W. Di Liu, Y. Chen, W. Hu, *Nano Res* **2022**, *16*, 4240.